JUN 2 2 2006

IN THE UNITED STATES PATENT AND TRADEMARK OFFICE

In re Application of:

Dorian Liepmann, et al

DNA SEQUENCING AND GENE
IDENTIFICATION

Serial No. 10/086,087

Filed 28 February 2002

Commissioner for Patents
P.O. Box 1450
Alexandria, VA 22313-1450

Sir:

Group Art Unit: 1634

Examiner: Thomas J. O'Farrell

I hereby certify that this correspondence is being
deposited today with the United States Postal
Service as first class mail in an envelope addressed
to Commissioner For Patents, P.O. Box 1450,
Alexandria, VA 22313-1450.

Christine Tolhurst
Christine Tolhurst

June 20, 2006
Date

DECLARATION UNDER 37 C.F.R. §1.131

1.   I, Zhihao Yang, declare that I received a degree of PhD in Chemistry from the
University of Wisconsin in 1998; I have been employed as a research scientist with
Eastman Kodak Company since August of 1998; I was employed in the development
of coatings for micro-electromechanical systems (MEMS) technology from 1998-
2003.

2.   I, Tiecheng A. Qiao, declare that I received a Bachelor of Science degree in
chemistry in 1986 from Jilin University, a Master of Science degree in chemistry in
1989 from Jilin University, and a PhD degree in Chemistry in 1995 from the
University of Rochester. I obtained postdoctoral training in biochemistry from MIT
from 1995-1997. I have been employed by the Eastman Kodak Company since 1997
and engaged since that time in the research and development of photographic paper,
nanotechnology, and biotechnology. I am a named inventor or co-inventor in issued
United States Patents related to my research and development activities.

3.   I, Susan J. Muller, declare that I received a degree of PhD in Chemical
Engineering from the Massachusetts Institute of Technology in 1986; I have been

BEST AVAILABLE COPY

employed as a faculty member in Chemical Engineering at the University of California, Berkeley, since 1991. I have been involved in research in polymer dynamics, fluid mechanics, and microfluidics at Berkeley. My involvement in microfluidics research and the behavior of DNA in microfluidic devices led to discussions with co-inventors Liepmann, Yang, and Qiao that led to this invention.

4.   I, Dorian Liepmann, declare that I received a degree of PhD in Applied Mechanics from the University of California, San Diego in 1990; I have been employed as a faculty member at the University of California, Berkeley since 1992. I have worked on microfluidic devices, MEMS and BioMEMS since 1995, and my work on biosensors and microfluidic valves and mixers led to collaborations with co-inventors Muller and Yang at Kodak.

5.   We are the co-inventor of the above-captioned patent application; and

6.   Chan et al. (Pre Grant Publication 2003/0059822, "Chan-1") and Hannah et al. (US Patent 6,767,731 B2) are asserted against the above-identified pending application under 35 USC §102(e).

7.   The claimed invention was conceived in the U.S. before the first U.S. filing date of either application, as evidenced by the attached notebook page 154, dated June 5, 2001 (European notation), recording a conversation between Zhihao Yang and Tiecheng A. Qiao. (See Attachment 1)

8.   The reference on the notebook page "as shown in Berkeley" refers to a published article "Effect of Flow on Complex Biological Macromolecules in Microfluidic Devices," by Polly S. Shrewsbury, Susan J. Muller, and Dorian Liepmann and published in 2001 in Biomedical Microdevices,3:3, 225-238 by Kluwer Academic Publishers. (See Attachment 2)
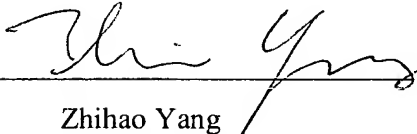
9.   After further consideration, we submitted our idea to the legal department of Eastman Kodak Company using a company tracking system, Invention Tracker. The idea was first recorded in Invention Tracker August 10, 2001, and was approved for patent application preparation August 27, 2001. (See Attachment 3)

10.   The application was then prepared in cooperation with the legal department, and filed on February 28, 2002.
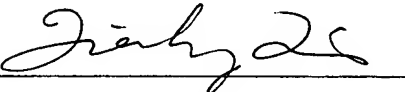
11.   The attached documents show that the invention was conceived in the U.S. before the earliest U.S. filing date of either Chan-1 or Hannah, and diligence was exercised in pursuing a patent application from the time of conception to the time of filing.

12.   The undersigned declare further that all statements made herein of the undersigned's own knowledge are true and all statements made on information and belief are believed to be true. These statements are made with the knowledge that willful false statements and the like so made are punishable by fine or imprisonment, or both, under section 1001 of Title 18 of the United States Code and that such willful false statements may jeopardize the validity of the application or any patent issuing thereon.
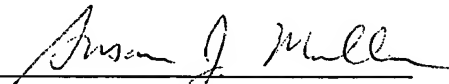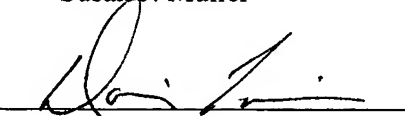
Date: June 5, 2006

Zhihao Yang

Date: June 7, 2006

Tiecheng A Qiao

Date: June 12, 2006

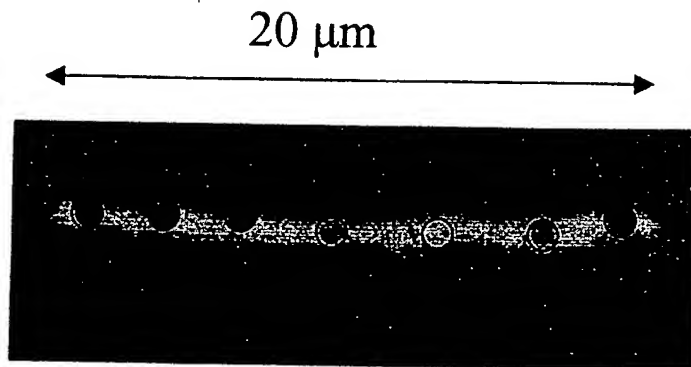Susan J. Muller

Date: June 12, 2006

Dorian Liepmann

Attachments: 1, 2 and 3

Single Molecular DNA Detection using Color-beads Labels

- ✗ Attack different oligo-nucleotides with different colored beads
- ✗ hybridize the labeled oligo-nucleotides with unknown DNA molecules
- ✗ stretch the DNA molecules from random coil to linear conformation under microscope by a microfluidic device as shown in Berkeley.
- ✗ record the order of colored-beads to determine the species of the DNA.

20 μm

Attachment #1   10/086,087

Effect of Flow on Complex Biological Macromolecules in Microfluidic Devices

Polly J. Shrewsbury,[1] Susan J. Muller,[2]*
and Dorian Liepmann[3]

[1]Bioengineering Program, [2]Department of Chemical Engineering,
and [3]Department of Bioengineering, University of California,
Berkeley, Berkeley, CA 94720

Abstract. Understanding the transport, orientation, and deformation of biological macromolecules by flow is important in designing microfluidic devices. In this study, epi-fluorescence microscopy was used to characterize the behavior of macromolecules in flow in a microfluidic device, particularly how the flow affects the conformation of the molecules. The microfluidic flow path consists of a large, inlet reservoir connected to a long, rectangular channel followed by a large downstream reservoir. The flow contains both regions of high elongation (along the centerline as the fluid converges from the upstream reservoir into the channel) and shear (in the channel near the walls). Solutions of λ-DNA labeled with a fluorescent probe were first characterized rheologically to determine fluid relaxation times, then introduced into the microfluidic device. Images of the DNA conformation in the device were captured through an epi-fluorescent microscope. The conformation of DNA molecules under flow showed tremendous heterogeneity, as observed by Chu [7,12] and co-workers in pure shear and pure elongational flows. Histograms of the distribution of conformations were measured along the channel centerline as a function of axial position and revealed dramatic stretching of the molecules due to the converging flow followed by an eventual return to equilibrium coil size far downstream of the channel entry. The importance of shear was probed via a series of measurements near the channel centerline and near the channel wall. High shear rates near the channel wall also resulted in dramatic stretching of the molecules, and may result in chain scission of the macromolecules.

Key Words. microfluidics, lab-on-a-chip, macromolecular conformation, hydrodynamics

Introduction

Microfabrication processes enable the design and manufacture of systems on the microscale. Such microsystems are capable of processing and analyzing biochemical samples and offer multiple advantages compared to conventional systems and protocols. Scaling down the system and increasing the number of samples processed per chip would result in heightened efficiency and reduced cost [1]. The realization of these benefits, however, requires understanding fundamental physical principles on this scale. Any change in conformation or stability accompanying the processing of a macromolecule in a microsystem must either parallel that which occurs during conventional laboratory testing, be benign to the end analysis, or be accounted for in the interpretation of data. Toward this goal, this work seeks to characterize the behavior of biological macromolecules during flow through a microdevice and to identify the critical parameters influencing this behavior.

A microflow composed of biological macromolecules constitutes a multi-faceted problem. Because of high surface to volume ratios in a microdevice, viscous forces dominate inertial forces and surface forces gain significance. Mathematically, Stokes flow and a vanishing Reynolds number describe the behavior of a Newtonian fluid on this scale [2–4]. The addition of biological macromolecules to a Newtonian solvent increases the complexity of fluid flow by causing non-Newtonian effects. For these fluids, viscosity may depend upon shear rate, and the behavior of the system is a function of the intrinsic properties of the polymer, on the solvent characteristics, and on the flow parameters. Two quantities predictive of non-Newtonian behavior are the polymer relaxation time λ, and the Deborah number De, a nondimensional parameter equal to the product of λ and shear rate γ: De $= \lambda\gamma$.

Flow through a microdevice is a combination of elongational flow and shear flow. Necessarily, the predominance of each flow type varies with position within the device. For example, shear flow dominates at the channel walls, and elongational flow is greatest at the channel center near channel contractions. Previous studies have experimentally recorded and have modeled the conformations of DNA molecules in both a pure elongational [5–9] and in a pure shear flow [10–12]. These studies reported the stretching of the macromolecule when subjected to either flow as a function of De and residence time in the flow. Given these findings, we expected to observe similar deformation of DNA molecules flowing through a more complex, nonhomogeneous flow in a silicon-fabricated microdevice. Here, we focus on the effects of the flow on the conformation of

---

*Corresponding author.

DNA. The effects of the DNA on the flow field are assumed negligible; this assumption will be probed in detail in a future study. Identifying the conditions conducive to deformation and the extent to which deformation occurs is relevant to designing a device and defining flow parameters that best support the stability and functional integrity of the macromolecule during the processing and analysis of biochemical samples.

Materials and Methods

Device fabrication

Fabrication begins with a n-type, 4 inch (1 0 0), single surface polished, silicon wafer (see Figure 1a). Wet oxidation of the wafer at 1100°C for 3 hours produces a 1 μm layer of silicon dioxide on the wafer's surface (1b). The first photolithography sequence defines placement of the device reservoirs and channel: 8 mm long, 300 μm wide (1c–1d). Development of the photoresist then allows an oxygen plasma etch of the exposed silicon dioxide (1e). The remaining silicon dioxide serves as a mask for a subsequent reactive ion etch of the device. The second photolithography sequence patterns the

wafer through-holes (1 mm diameter) located in the device reservoirs (1g–1h). These through-holes function as fluidic inlets and outlets and are formed from a deep reactive ion etch, or DRIE (1i). The application of 10 μm of photoresist during the second lithography step protects the areas of the wafer not etched during DRIE. Removal of the photoresist (1j) permits a reactive ion etch of the device features. The depth of these features (reservoirs and channel) is a function of etch time, and for this device equals 60 μm (1k). Finally, dipping the wafer in buffered hydrofluoric acid removes the remaining silicon dioxide from the wafer (1l). The devices can then be separated by dicing with a diamond saw.

Device bonding and fluidic connection

The ability of a microscope to resolve DNA molecules through a glass coverslip depends upon the thickness of the glass coverslip and on the magnification of the microscope. An objective magnification of 100 × limits the glass thickness to 0.17 mm. In order to effectively bond this thickness of glass to a device, a bonding protocol using epoxy was developed. First, a spinner was used to uniformly apply epoxy to a coverslip. The epoxy was then cured at 90°C for 45 minutes. To ash epoxy
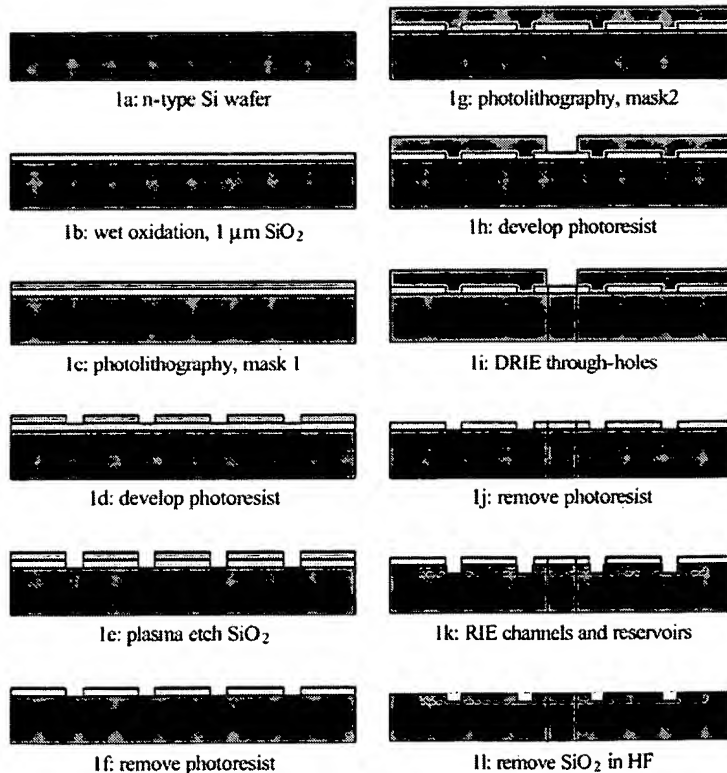

Fig. 1. Schematic of the microfabrication process.

from the device reservoirs and channel, an oxygen plasma was directed through the device via the device through-holes. Inspection of the device with a microscope confirmed the epoxy removal. Polyvinyl tubing was then affixed to the through-holes, located at the proximal ends of both reservoirs, with epoxy. This last step completed the fluidic path, and flow through the device could be mechanically controlled with a syringe pump.

DNA visualization

The biological macromolecule studied in these experiments was λ-DNA (New England Biolabs). The molecular weight of this DNA is 31.5×10^6 Daltons, which corresponds to 48,502 base pairs. Selection of this DNA for experimentation stemmed from two factors: First, the contour length of the DNA is long, which increases the likelihood for detecting any changes in its conformation. Second, within the literature there exists substantial documentation of the structure of this molecule and of alterations in this structure which occur when labeling the DNA with a fluorescent probe for purposes of visualization [13–16].

As per former researchers, the probe chosen to visualize the DNA was YOYO-1 (Molecular Probes) at a dye : base pair ratio of 1 : 5. YOYO-1 intercalates within the DNA backbone and effectively stiffens and lengthens the molecule. Incubation of the DNA and probe occurred for a minimum of 2 hours at room temperature. For incubation with YOYO-1 and for experimentation, the DNA was isoionically diluted in a pH 8 buffer consisting of 10 mM tris-HCl, 2 mM EDTA, 10 mM NaCl. Due to the sensitivity of the dye-DNA complex to light and to oxygen radicals, all incubation and experiments occurred in the dark and the oxygen scavenger B-mercaptoethanol was added to the buffer solution at a final concentration of 4% (v/v), respectively. The bulk viscosity of the solution was adjusted as indicated by adding sucrose.

Imaging instrumentation

For all imaging experiments, an Olympus IX70 inverted epifluorescence microscope equipped with a 100 × / 1.3 NA Universal Plan Fluorite oil immersion objective and a high pressure 100 W, 20 V Mercury burner as the illumination source was used. A fluorescence cube from Chroma containing the following optical filters was used with the probe YOYO-1: excitation 460–500, long pass beamsplitter 505, emission 510–560. A high-gain image intensifier (KS-1381 Videoscope International, Ltd.) coupled the microscope to a high performance monochrome CCD camera (4900 series Cohu). Data was recorded to S-VHS video using a S-VHS Mitsubishi VCR. The maximum image capture rate was 30 frames/second. Images were transferred from video to computer using a Scion framegrabber and NIH Image software. Image analysis was performed on a Macintosh G3.

DNA rheology

The rheological characterization of λ-DNA was performed using a Vilastic 3 Viscoelasticity Analyzer from Vilastic Scientific, Inc. The instrument produces an oscillatory flow in a capillary and measures the pressure and volumetric flow rate, allowing the determination of both the viscous and elastic response of a fluid sample. The Vilastic 3 was interfaced with and controlled by a PC containing a Pentium II processor. Data were recorded with the Vilastic 3 operating in high drive at a frequency of 2 Hz. The drive level was swept from 1 to 10. The inner radius and length of the Vilastic 3 measurement tube were 0.0508 cm and 6.381 cm, respectively. Distilled water served as the coupling fluid. A Haake K10 circulator attached to the thermal jacket encasing the measurement tube regulated the temperature of the sample being measured. All DNA samples were diluted as described above and were maintained at a constant temperature of 23°C.

Experiment

Characterization of microfluidic device

The scanning electron micrographs in Figure 2 illustrate the microfluidic device geometry in which the DNA conformation was imaged. The device shown reflects alterations from a previous prototype in that there is a single fluidic path (i.e., only one channel) and the inner edges of the device are rounded. Experiments demonstrate that these changes ease monitoring of flow uniformity and facilitate the removal of trapped air within the device. For notation purposes, x represents the direction of flow, y is the channel depth, and z is the channel width. An important design feature is the narrowing of the fluidic path from the reservoir into the channel which forms a contraction and produces an elongational flow. In the present work, we focus on the effects of flow on DNA conformation. The effect of the DNA on the flow field is assumed negligible and the velocity and stress fields are assumed to be identical to those of a Newtonian fluid.

For a Newtonian fluid of viscosity η flowing in a rectangular channel, velocity and shear stress profiles in the $y = 0$ plane for a channel having cross-sectional dimensions of 300 μm × 60 μm appear in Figure 3. These represent exact solutions to the equations of motion [17]. The solutions for the fully-developed axial velocity $u(y, z)$ and volumetric flow rate Q in terms of the axial pressure gradient dP/dx are:
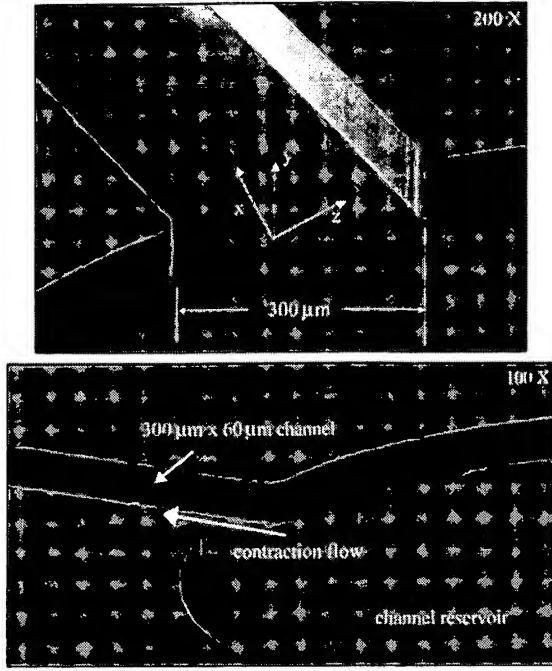
Fig. 2. SEMS of microfluidic device showing channel entrance and reservoir.

$$u(y,z) = \frac{16a^2}{\eta\pi^3}\left(-\frac{dP}{dx}\right)\sum_{i=1}^{\infty}(-1)^{\frac{(i-1)}{2}}\left[1 - \frac{\cosh(i\pi z/2a)}{\cosh(i\pi b/2a)}\right]\frac{\cos(i\pi y/2a)}{i^3}$$

$$(1)$$

$$Q = \frac{ba^3}{6\eta}\left(-\frac{dP}{dx}\right)\left[1 - \frac{192a}{\pi^5 b}\sum_{i=1}^{\infty}\tanh\frac{(i\pi b/2a)}{i^5}\right] \qquad (2)$$

where i is an integer, $-b<z<b$ and $-a<y<a$. To obtain the shear stress, the pressure gradient dP/dx as a function of Q was determined from equation (2) and substituted into the expression for $u(y,z)$. The product of the derivative of the velocity $u(y = 0, z)$ with respect to z and the viscosity yields shear stress τ_{xz} in the $y = 0$ plane. Equations (1) and (2) can be used to calculate the local shear rate and De within the microfluidic device. These profiles illustrate that the velocity is greatest at the center of the channel, and the shear stress is greatest at the wall of the channel. In contrast to the parabolic profiles characteristic of pipe flow, the high width to height aspect ratio of this rectangular geometry results in plug-like flow in the central plane; i.e., drastic changes in velocity and shear stress occur within close proximity (of order 30 µm) to the channel walls. The velocity profile along the smaller, transverse direction, $u(y,z = 0)$ is nearly parabolic.

Characterization of relaxation time for λ-DNA

A natural coupling exists between the fluid mechanics within a microdevice and the behavior of the biological macromolecules flowing through the device. λ-DNA exhibits viscoelasticity, and identification of its relaxation time λ contributes to understanding this coupling. Using the Vilastic 3, the viscosity of dilute solutions of DNA was measured. This instrument, unlike traditional rheometers, employs a piston to force fluid within the measurement tube into an oscillatory flow. A nylon membrane separates a piston surrounded by silicone oil from the coupling fluid (distilled water) in the device chamber and from the test fluid in the measurement tube. Because the machine lacks moving parts, frictional effects are avoided.

During oscillatory flow, the instrument measures the pressure gradient along the measurement tube and the volume flow through the measurement tube. Knowledge of these and additional variables including the operating frequency and the measurement tube dimensions allows calculation of shear stress, shear rate, and shear strain at the tube wall. Determination of the viscosity (or, more accurately, the complex viscosity since the flow is oscillatory, rather than steady) readily follows from the ratio of shear stress to shear rate.

The relationship between concentration and viscosity for λ-DNA in a 15 centipoise buffered solution appears in Figure 4. The viscosity of the buffer is also shown. By fitting the concentration dependence of the viscosity η, the intrinsic viscosity [η] of the molecule can be calculated. The intrinsic viscosity [η] is related to the solvent viscosity η_{solv} and the solution concentration c by:

$$\eta = \eta_{solv}\left(1 + [\eta]c + k_1[\eta]^2c^2 + \cdots\right) \qquad (3)$$

where k_1 is the Huggins constant. The Huggins constant depends on temperature and on the particular macro-molecule-solvent system, and typically has a value in the range of 0.3–0.5. Defining the specific viscosity η_{sp} as:

$$\eta_{sp} = \frac{(\eta - \eta_{solv})}{\eta_{solv}} \qquad (4)$$

and substituting for η_{sp} yields the equation:

$$\frac{\eta_{sp}}{c} = [\eta] + k_1[\eta]^2c + \cdots \qquad (5)$$

The ratio of specific viscosity to concentration is termed the reduced viscosity. Plotting this value against concentration in the low concentration limit produces a y-intercept equivalent to the intrinsic viscosity (Figure 5). The nonlinearity of the data in Figure 5 at very low concentrations is due to the changing ionic
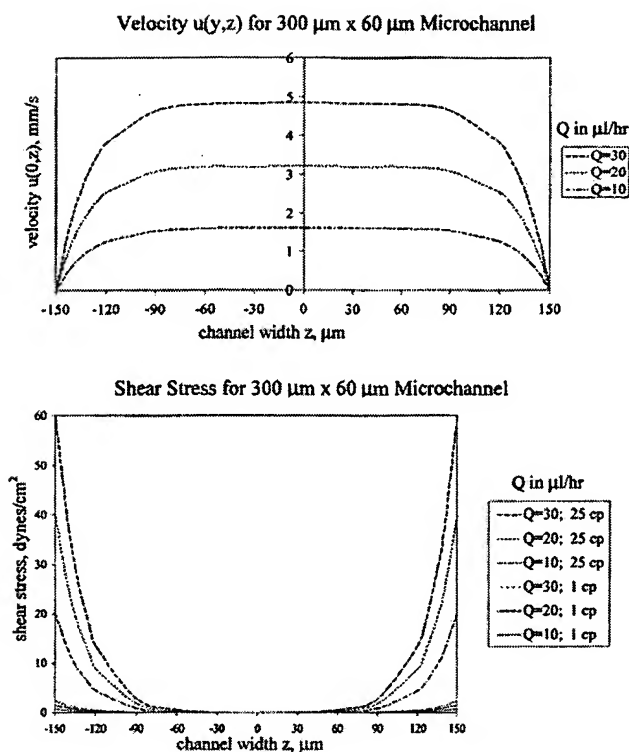
Velocity u(y,z) for 300 μm x 60 μm Microchannel

Shear Stress for 300 μm x 60 μm Microchannel

Fig. 3. Profiles for the fully-developed velocity $u(y = 0, z)$ and shear stress τ_{xz} in the $y = 0$ plane in the channel flow of a Newtonian fluid.

strength of the solution. The ionic strength decreases with DNA concentration and the DNA expands in the absence of charge-shielding. Taking the linear, higher concentration data to represent the behavior of the buffered DNA in solution as a flexible coil, the Rouse model yields the relaxation time λ, as:

$$\lambda = \frac{[\eta]\eta_{solv}M}{RT} \tag{6}$$

where M is the molecular weight of λ-DNA, R is the gas constant, and T is temperature. From this process, the intrinsic viscosity was calculated as 3530 ml/g. The corresponding relaxation time in a 15 centipoise sucrose buffered solvent is then 0.68 second. Since relaxation time scales with viscosity, for λ-DNA in a buffered solvent at 0.904 centipoise the relaxation time λ is 0.041 second.
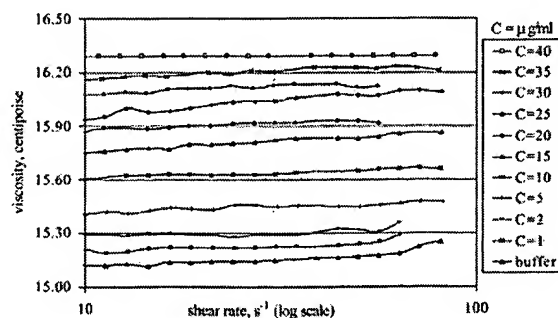
Fig. 4. Viscosity as a function of concentration and shear rate for a buffered solution of λ-DNA. The viscosity of the buffer was adjusted to roughly 15 centipoise through the addition of sucrose.
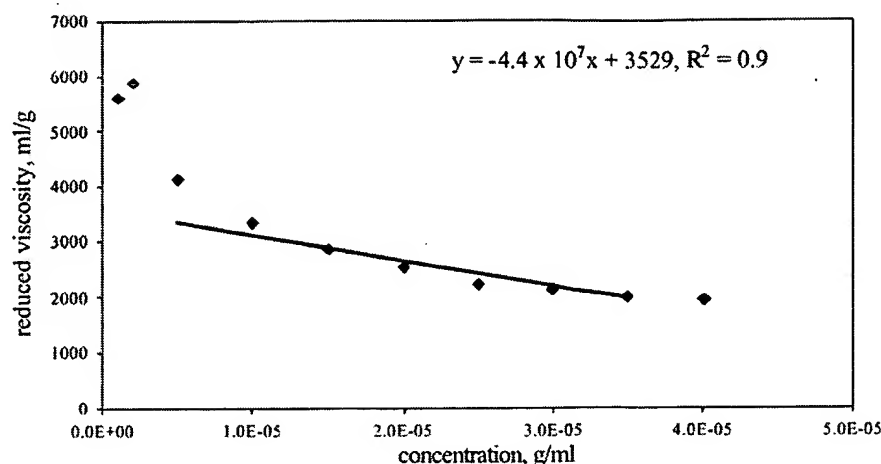
Fig. 5. *Calculation of the intrinsic viscosity of the DNA in solution. The extrapolation of the high concentration data for the reduced viscosity to the y-axis provides an estimate of the intrinsic viscosity [η]. R^2 is the square of the correlation coefficient.*

Characterization of DNA Behavior in a Microfluidic Flow

As a first attempt at understanding how λ-DNA behaves in a microfluidic flow, λ-DNA molecules were visualized at 100 × magnification flowing though the center of a microchannel. The molecules were imaged downstream of the channel entrance, at a distance approximately one third the total channel length from the entrance (Figure 6). At this location, the flow profile is fully developed and lacks entrance effects. The viscosity of the buffered solvent was 1 centipoise and the concentration of the DNA was 0.30 μg/ml. The overlap concentration, c^*, at which the macromolecules completely fill space without overlapping, can be estimated from the rheological data as

$$c^* = \frac{1}{[\eta]} = 283 \frac{\mu g}{ml} \qquad (7)$$

Hence the solution under study, at $c \cong 0.001\, c^*$, is dilute.
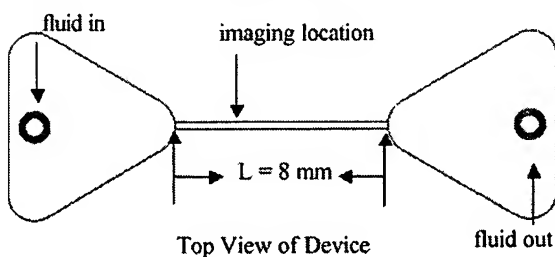
Fig. 6. *Schematic of device and imaging location for the experiments reported in Figures 7–9.*

For this experiment, images of molecules were captured for flow rates ranging from 0 μl/hr to 30 μl/hr. All other variables were constant. At each flow rate, a minimum of 100 molecules was imaged and their lengths, as projected onto the direction of flow (x), were measured in pixels. Magnification at 100 × of a reticle having micron divisions permitted conversion from pixels to microns.

Sample images of λ-DNA at each flow rate appear in Figure 7. Shown with each flow rate is the maximum Deborah number (De) existing within the channel for the respective experimental conditions; that is, the Deborah number used here is based on the wall shear rate. Since imaging of the molecules occurred at the channel centerline, where the shear rate tends to zero, the observed response of the molecules was not this extreme. Because, however, the imaging area spanned about 20 microns and because focusing with an epifluorescence microscope is not exact, the conformation of these macromolecules realistically reflects exposure to a low shear flow.

Also shown for reference are fluorescent beads. At high flow rates, travel of the molecules may exceed the camera capture rate of 30 frames/sec. An optical artifact or streaking of the molecules and beads ensues. Imaging beads allows detection and quantification of any streaking.

The DNA molecules imaged in Figure 7 seemingly elongate along streamlines at increasing flow rates and Deborah numbers. Comparison of these images to fluorescent beads, however, reveals that streaking obscures any stretching as the beads follow the same pattern as the DNA. Thus, further attempts to determine
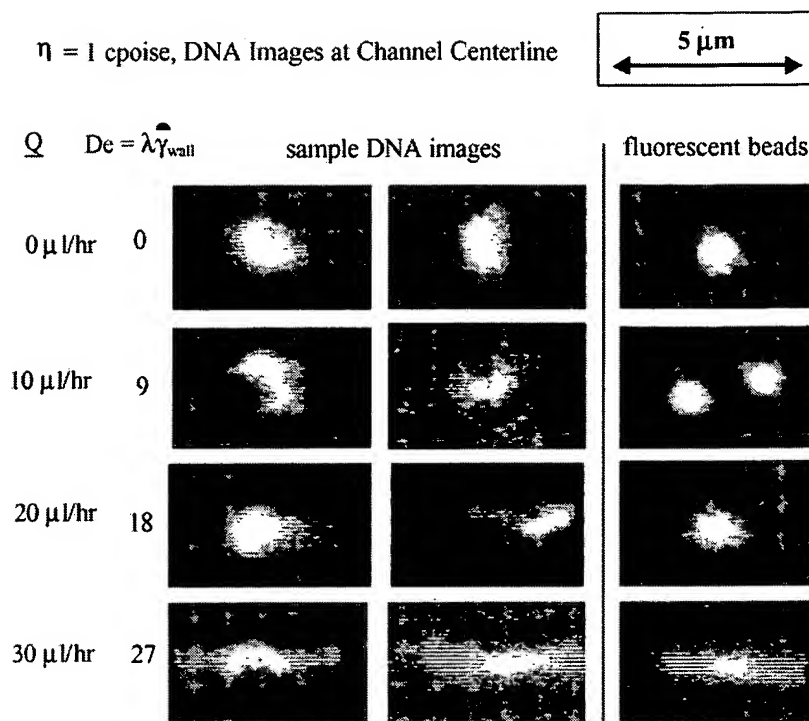
Fig. 7. *Sample images of DNA and fluorescent spheres flowing through the microchannel as a function of flow rate. The imaging location is indicated in Figure 6. The viscosity of the buffer solution is 1 centipoise.*

the effects of flow on the conformation of the macromolecules in this solution cannot involve increasing flow rates given the existing experimental set-up.

One alternative method for increasing the stress imposed on the molecule while circumventing optical streaking is to increase the solution viscosity. Repeating the experiment in a buffered solvent with a viscosity of 25 centipoise produces the sample images in Figure 8. These images reveal that λ-DNA can undergo dramatic stretching in a microfluidic flow. Increasing the solvent viscosity increased the relaxation time of the molecule, and dramatic changes in conformation could be observed at flow rates where streaking is essentially negligible. Compare, for example, the images in Figure 8 of the beads and of the DNA at a flow rate of 20 µl/hour.

The histogram in Figure 9 contains the percent frequency of all recorded molecular lengths. For all flow rates, a broad distribution of DNA lengths exists. At 10 µl/hour, the majority of molecules occupy a coiled state. The molecules elongate at 20 µl/hour, and the histogram for this data set shifts to the right. By 30 ml/ hour, the data histogram looks somewhat bi-modal, and the variation in recorded lengths is the most extreme. The appearance of a greater number of molecules having

lengths between 2 µm and 3 µm at 30 µl/hour relative to 20 µl/hour may reflect chain scission.

The molecular deformation observed may be attributable to a combination of elongational and shear flow. At the channel centerline, the shear rates should be extremely low and, at the imaging location, the elongational channel entrance effects should have partially dissipated. Thus, two experiments to elucidate the relative contribution of each type of flow to the observed effects logically follow. The first experiment examines the elongational flow along the channel centerline, and the second explores the shear flow at the channel wall.

Elongational Flow Effects

An elongational flow exists at the channel centerline; the fluid accelerates as it enters the channel from the upstream reservoir and decelerates as it exits the channel into the downstream reservoir. Therefore, imaging DNA molecules moving along the centerline of the device lends insight into the impact of a converging and diverging flow on molecular conformation and identifies the positions within the device most likely to produce deformation of macromolecules. By using the fine focus
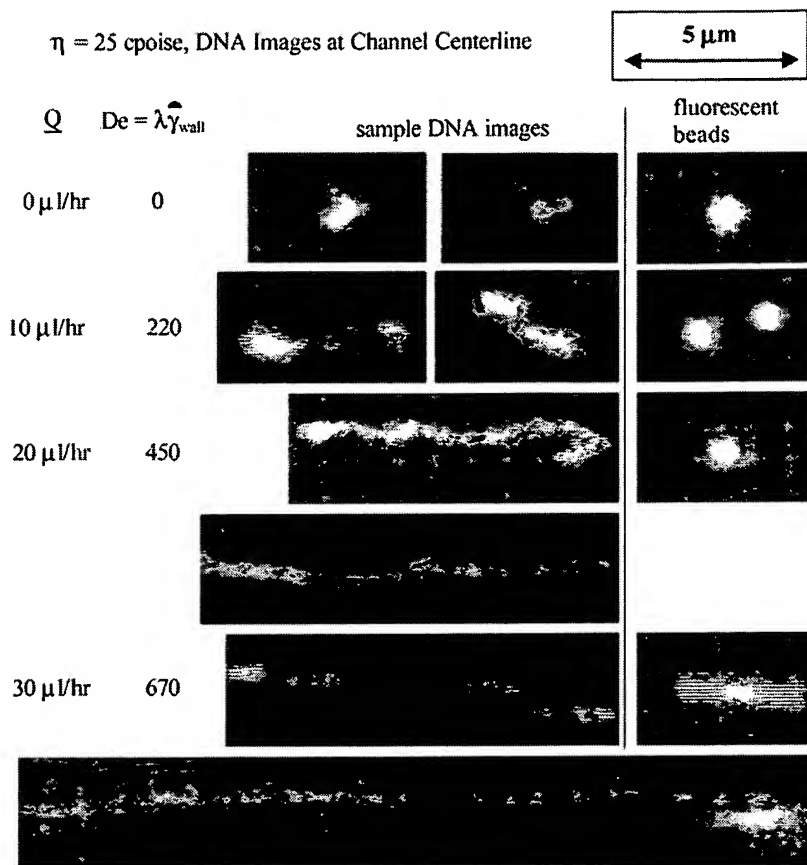
η = 25 cpoise, DNA Images at Channel Centerline

5 μm

Q   De = $\lambda \dot{\gamma}_{wall}$ sample DNA images   fluorescent beads

0 μl/hr   0

10 μl/hr   220

20 μl/hr   450

30 μl/hr   670

Fig. 8. *Sample images of DNA and fluorescent spheres flowing through the microchannel as a function of flow rate. The imaging location is indicated in Figure 6. The viscosity of the buffer solution is 25 centipoise.*
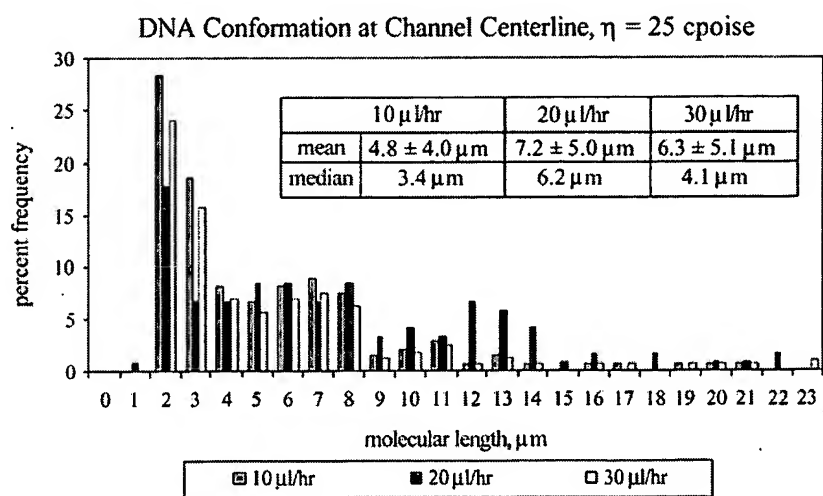
DNA Conformation at Channel Centerline, η = 25 cpoise

percent frequency

	10 μl/hr	20 μl/hr	30 μl/hr
mean	4.8 ± 4.0 μm	7.2 ± 5.0 μm	6.3 ± 5.1 μm
median	3.4 μm	6.2 μm	4.1 μm

molecular length, μm

⊡ 10 μl/hr   ■ 20 μl/hr   □ 30 μl/hr

Fig. 9. *Histograms of the projected length of the DNA flowing through the microchannel. The imaging location and viscosity are those indicated in Figure 8. A minimum of 100 molecules was recorded at each flow rate.*

Imaging Locations: A-F

fluid out

A   B   C   D E   F

L = 8 mm

fluid in

A
B
C
D
E
F

sample A-DNA images
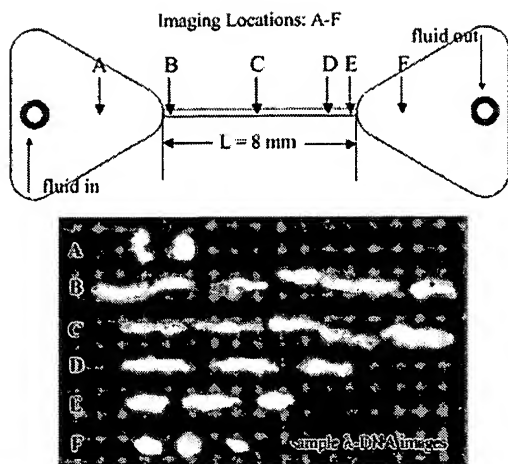
Fig. 10. DNA conformation along the channel centerline as a function of axial position in the device. The representative images indicate the dramatic stretching of the molecule due to the elongational flow at the channel entrance, and the recovery of its equilibrium conformation as it travels through the channel and into the downstream reservoir.

of the microscope to locate the top and then bottom of the device (approximately 0.6 μm/division), the channel centerline was found. As illustrated in Figure 10, the imaging position varied along x, the direction of flow, while the y and z positions remained constant. The concentration of DNA in buffered solution was 0.3 μg/ml, the viscosity was 15 centipoise, and the flow rate was 5 μl/hour.

At A, the DNA molecule is in the device reservoir. The shape, as represented by the sample images in Figure 10, is coiled. Having fully entered the channel at B and having just undergone a converging flow, the DNA molecules are highly elongated. Dividing flow rate by the device cross-sectional area gives a mean fluid velocity of 0.077 mm/sec. within the channel. In this 15 centipoise viscosity solution, the relaxation time of the molecule is 0.682 sec. Therefore, in traveling 0.053 mm along the centerline, only about one relaxation time will have elapsed, and a large fraction of the elongational stress from entering the channel will not yet have relaxed. At position C, the approximate midpoint of the 8 mm channel, the DNA molecules as seen in the sample images are still not entirely relaxed. Greater relaxation of the molecule is observed further downstream of the channel entrance, at positions D and E. Not until the molecule exits the channel at F, however, does the molecule recover the conformation observed at A.

Figure 11 is a histogram of the lengths of all DNA molecules measured at positions A–F. A minimum of 100 molecules was recorded for each position. As seen

with the sample images in Figure 10, the DNA molecules elongate in the contraction flow at the channel entrance (B). Only after exiting the channel at F do the molecules return to a relaxed, coiled conformation observed in the device entrance reservoir at A. To ensure optical streaking did not bias these measurements, fluorescent beads were imaged under identical flow conditions experienced by DNA molecules; these data are reported in Table 1.

Since the confidence intervals for the bead lengths overlap, streaking of the molecules is not a concern.

This experiment demonstrates that an elongational flow in a microfluidic device can cause DNA molecules to stretch, and that the time required for the molecules to recover their initial conformation exceeds the relaxation time by a large (of order 100) factor. The data suggests that an understanding of the fluid relaxation time and the detailed kinematics is critical when designing microfluidic devices. Without this knowledge, the placement of too many stresses in series will stretch and degrade the molecules and will bias any analysis.

Shear Flow Effects

Having examined the elongational flow along the channel centerline, the next step is to study the shear flow along the channel wall. Figure 12 shows the imaging positions for this flow experiment. Molecules were imaged at the channel wall and near the channel centerline. The "upstream" wall location immediately follows the channel entrance, and the "downstream" location precedes the channel exit. At the channel wall upstream, the channel wall downstream, and near the channel centerline, images were recorded at 5 depths (in y): at 6 μm, 12 μm, 30 μm, 48 μm, and 54 μm from the top channel surface. The total channel depth was 60 μm. The top and bottom of the channel were located as previously described. In these experiments the DNA concentration was 0.3 μg/ml, the solution viscosity was 42 centipoise, and the flow rate was 5 μl/hour. Figures 13–15 contain histograms of the molecular lengths of DNA projected onto the direction of flow. A minimum of 100 molecules was measured at each depth. To facilitate a quick comparison among depths, the median molecular length is reported in the upper right corner. As previously, fluorescent beads were imaged to ensure optical streaking did not bias the measured lengths of the molecules. These results are summarized in Table 2.

The effects of shear flow on DNA conformation can be observed by examining the histograms in Figure 13 which represent different vertical locations near the channel centerline. As indicated in Figure 3, the shear rate is highest near the top and bottom walls and

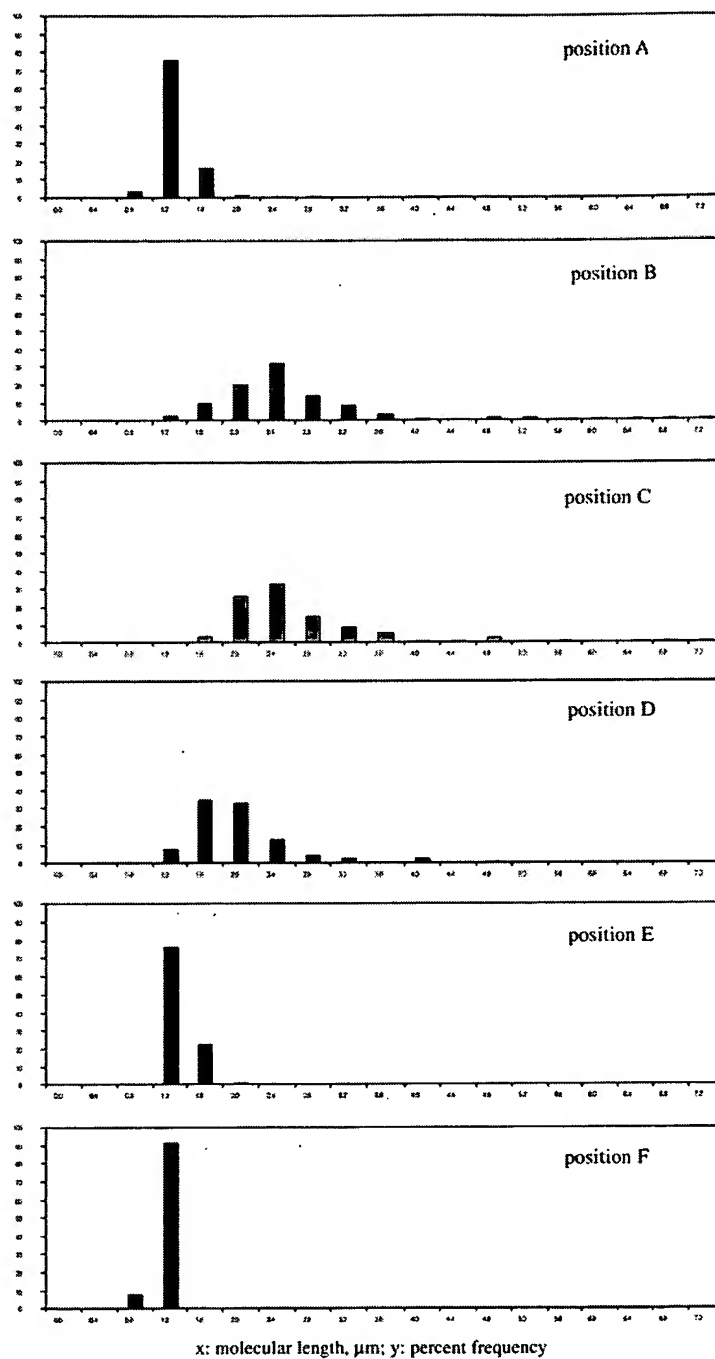x: molecular length, μm; y: percent frequency

Fig. 11. Histograms of projected lengths of DNA on the channel centerline as a function of axial position in the device. The positions are indicated in Figure 10. A minimum of 100 molecules was recorded at each position.

Table 1. Bead lengths at channel center

Flow Rate	Bead length in direction of flow (x)
0 µl/hour	1.00 ± 0.10 µm
5 µl/hour	1.05 ± 0.08 µm

Number of Beads Measured $N = 60$
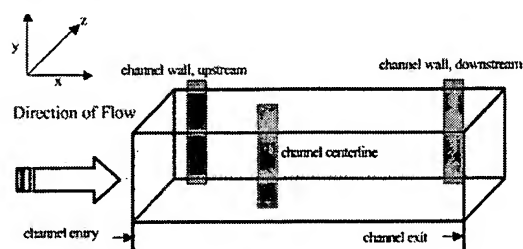
Fig. 12. Imaging positions for the flow experiments reported in Figures 13–15.

approaches zero at the channel midplane $(y = 30\,\mu m)$. This is clearly reflected in·increased stretching of the molecules near the top and bottom of the channel, and relatively little stretching, and a much narrower distribution of conformations, near the midplane. Any residual deformation of the molecules due to the elongational flow associated with the contraction flow is modest relative to the deformation induced by shear at the walls for these conditions. Theoretically, the shear rate at equal distances from the channel midplane is identical. Therefore, the distribution of molecular lengths at 6 µm and 12 µm should mirror that at 54 µm and 48 µm, respectively. Differences may arise from dissimilar surfaces at the channel top (glass) and channel bottom (silicon) or from the limited sample size (> 100 molecules per depth).

Figure 14 shows the distributions of molecular lengths at different vertical locations near the upstream wall. Due
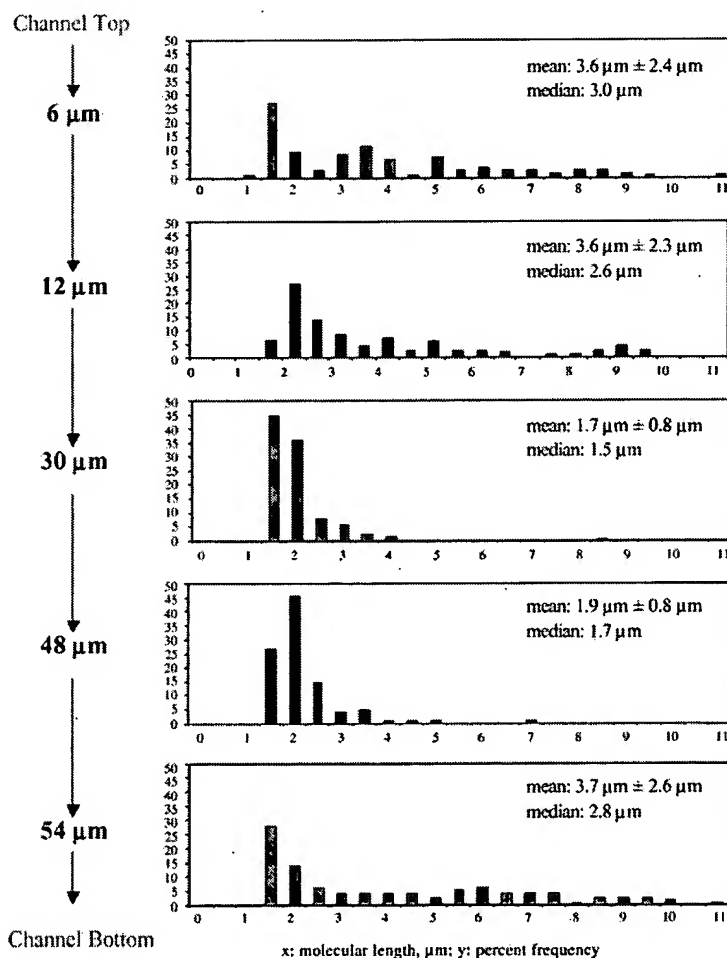
Fig. 13. Histogram of DNA conformations as a function of depth at the channel centerline location indicated in Figure 12. A minimum of 100 molecules was recorded at each position.
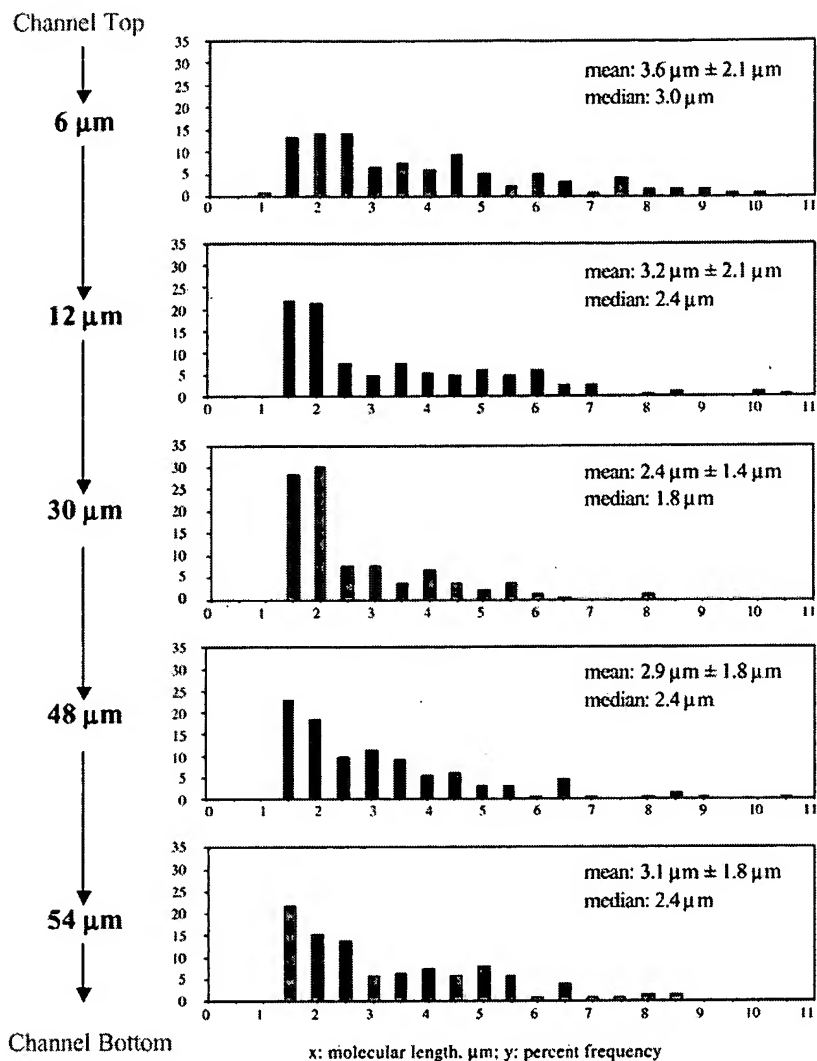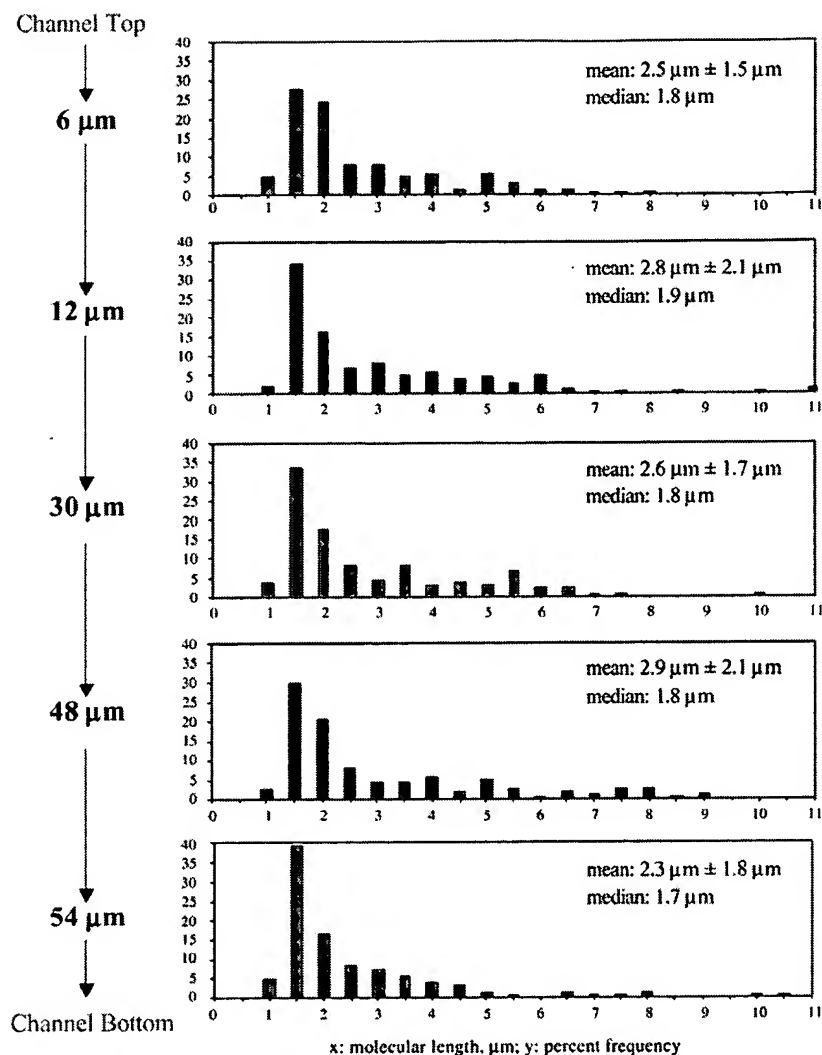
Fig. 14. Histogram of DNA conformations as a function of depth at the upstream wall location indicated in Figure 12. A minimum of 100 molecules was recorded at each position.

the presence of the top and bottom surfaces, the shear rate is again highest at these surfaces and decreases—but remains high—near the channel midplane. The histograms at all vertical locations are much more similar in shape and breadth than those in Figure 13. In particular, comparison of Figures 13 and 14 reveals that the molecules are much more stretched, and the histograms are much broader, near the midplane of the channel at the wall location than close to the centerline. Comparison of the two locations at $y = 30\,\mu m$ is perhaps the most compelling: near the channel center the histogram is very narrow and the mean length is $1.5\,\mu m$; at the wall a much

broader spectrum of lengths is observed and the mean length is $1.8\,\mu m$.

Figures 14 and 15 reveal a disparity between the distributions of DNA lengths at corresponding depths near the wall, but at different axial positions within the channel. At the downstream wall position, the histograms are essentially similar at all vertical positions within the channel; the hint of a second maximum in the histograms in Figure 14 is missing in Figure 15, and the population of longer molecules is smaller. In fact, at the positions nearest to the top and bottom walls, the median DNA length has dropped from 3 and $2.4\,\mu m$

Channel Top

6 µm

12 µm

30 µm

48 µm

54 µm

Channel Bottom

x: molecular length, µm; y: percent frequency

Fig. 15. Histogram of DNA conformations as a function of depth at the downstream wall location indicated in Figure 12. A minimum of 100 molecules was recorded at each position.

Table 2. Bead lengths for shear flow conditions

Channel position	Bead length in direction of flow (x)
channel wall 6 µm	1.01 ± 0.11 µm
channel wall 30 µm	1.04 ± 0.08 µm
channel wall 54 µm	0.88 ± 0.10 µm
channel center 6 µm	0.99 ± 0.09 µm
channel center 30 µm	1.05 ± 0.09 µm
channel center 54 µm	0.89 ± 0.08 µm

$q = 5$ µl/hr,
$\eta = 42$ centipoise

upstream to 1.8 and 1.7 µm at the downstream location. The decrease in median length with axial distance suggests that the DNA is undergoing chain scission in this high shear flow, and that the molecules are being irreversibly degraded. This hypothesis is currently under study in our laboratory.

Conclusion

The intent of this work was to characterize the behavior of biological macromolecules during flow through a microdevice. Through microscopy studies of the flow of

λ-DNA molecules in a simple microchannel connected to inlet and outlet reservoirs, we have observed dramatic changes in the molecular conformation due to flow. Both the elongational flow near the channel centerline (caused by the contraction from the reservoir to the channel) and the shearing flow near the walls resulted in profound stretching of some of the molecules, and a broadening of the distribution of conformations was observed. In addition, exposure to extended shearing may lead to chain scission—i.e., an irreversible change in the molecules. The extent to which the conformation of the molecules is affected by the flow is influenced by the device geometry, the solution viscosity, the flow rate, and the relaxation time of the solution. The Deborah number, a dimensionless parameter describing the importance of elasticity in the flow, has been used in this initial attempt to identify important effects. Higher De flows result in increased stretching of the molecules, longer times for the molecules stretched along the channel centerline to recover their initial conformation, and likely result in increased molecular degradation through chain scission.

Acknowledgments

References

1. M. Freemantle, Chemical and Engineering News **77**(8), 27–36 (1999).
2. J.P. Brody, P. Yager, R.E. Goldstein, and R.H. Austin, Biophysical Journal **71**, 3430–3441 (1996).
3. P. Graveson, J. Branebjerg, and O. Jenson, Journal of Micromechanical Microengineering **3**, 168–182 (1993).
4. C. Ho and Y. Tai, Annual Review in Fluid Mechanics **30**, 579–612 (1998).
5. P.S. Doyle, E.S.G. Shaqfeh, G.H. McKinley, and S.H. Spiegelberg, Journal of Non-Newtonian Fluid Mechanics **76**, 79–110 (1998).
6. R.G. Larson, J. Hu, D.E. Smith, and S. Chu, Journal of Rheology **43**(2), 267–304 (1999).
7. T. Perkins, D. Smith, and S. Chu, Science **276**, 2016–2021 (1997).
8. H. Reese and B. Zimm, Journal of Chemical Physics **92**(4), 2650–2662 (1990).
9. D.E. Smith and S. Chu, Science **281**, 1335–1340 (1998).
10. P. LeDuc, C. Haber, G. Bao, and D. Wirtz, Nature **399**, 564–566 (1999).
11. J.S. Hur, E.S.G. Shaqfeh, and R.G. Larson, J. Rheol. **44**, 713–742 (2000).
12. D.E. Smith, H.P. Babcock, and S. Chu, Science **283**, 724–727 (1999).
13. B. Akerman and E. Tuite, Nucleic Acids Research **24**(6), 1080–1090 (1996).
14. C. Bustamante, T.W. Houseal, D.A. Beavh, and M.F. Maestre, Journal of Biomolecular Structure and Dynamics **8**(3), 643–655 (1990).
15. S. Gurrieri, S.B. Smith, K.S. Wells, I.D. Johnson, and C. Bustamante, Nucleic Acids Research **24**(23), 4759–4767 (1996).
16. T.W. Houseal, C. Bustamante, R.F. Stump, and M.F. Maestre, Biophysical Journal **56**, 507–516 (1989).
17. F.M. White, *Viscous Fluid Flow* (McGraw-Hill, New York, 1974).

Invention Tracker

Eastman Kodak Company Restricted
Prepared For Patent Attorney

Kodak

Status	Action	Idea #	Docket #	Submitting Inventor	Title
Complete	Pursue Patent	SIS-1026	83426	Zhihao Yang	Single Molecular DNA Sequencing or Decoding

★ ....All star fields are required.............

Step 1 - Inventor : Idea Submission

★ IP Portfolio Code: 23 - Health Imaging Equipment 🔽   ❓

★ Cluster Coord Code: SIS - Donna Rankin-Parobek - Molecular Imaging 🔽

Idea #: SIS-1026   Idea Entry Date: 08/10/2001

Title: **Single Molecular DNA Sequencing or Decoding**

★ Submitting Inventor: Zhihao Yang/486108/US/EKC 🔽

Other Kodak Inventors: Tiecheng A. Qiao/436337/EKC
[Add Name] [Remove Name]

Other Inventors: Susan J. Muller, Dorian Liepmann

Is this idea entry originating in Europe ? ○ Yes ● No

Are any inventors on this Idea Non-US Citizens: ● Yes ○ No
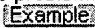
Inventor Name: Zhihao Yang

Country: China

★ Earliest Date of Invention: 06/05/2001 **(a)**

Notebook # / Page # / Other:

Description of Invention

Answer following questions and/or attach document

★ With regard to what project or product was your invention made?

★ What problem does the invention solve?

★ How does the invention solve the problem?

★ Data that shows how the invention solved the problem:
[Example]

★ Best mode known of practicing the invention:
[Example]

★ Describe how others tried to solve the

problem (Type or Attach Prior Art)?

●

★ What other products might this invention
be useful for?

★ Has the invention been disclosed to the ○ Yes ○ No
public or offered for sale?

★ Are you currently working with an ○ Yes ● No
Attorney on this invention?

When complete, click "SEND" an e-mail will [Send]   Date 08/10/2001
be sent to IPCoordinator for approval: Sent:

Step 2 - IP Coordinator : Idea Approval

Step 3 - Patent Legal Staff : Docketing/Patentability Meeting

Step 4 - IP Coordinator and Inventor : Attorney Ready Action Items

Step 5 - Patent Legal Staff : Confirmation and Filing

Step 5A - Attorney

Step 5B - PLA

★ Application Mail 02/28/2002(d)
Date:

External Attorney   Phon
Name: e:

Input the following info into IPMaster

Val # at Filing:	0508051 065
Attorney Ready Date:	02/28/2002 (c)

Click on the button to copy the row item to the clipboard

Add final "Application Filed" document to the bottom of the Invention Form in a .pdf format

When complete, click SEND. An e-mail will inform IF [Send] or ar Date Se 04/26/2002
Inventor that initial f   iplete:

Step 6 - IP Coordinator : Confirm IP Evaluation and Foreign Filing

Info from Step 1 and 6 (Prior to 10/01/2004)

Who can View and Edit this Document

Attachments and Comments

Comments:
To be co-filed with IJP-1239 under MEMS devices

Attachments:

Docket83426.doc Figure1.doc Figure2.doc Figure3.doc Figure4.doc DNA_Beads.ppt

Kodak_-_DNA_sequencing.p DNA_sequencing_-_Kodak.dc